



OPEN ACCESS

EDITED BY

Cheng-Kung Cheng, Shanghai Jiao Tong University, China

Rongshan Cheng, Shanghai Jiao Tong University, China Xiao Z...

China Institute of Sport Science, China

*CORRESPONDENCE Jing-Lai Xue,

[‡]These authors have contributed equally to this work

RECEIVED 15 March 2025 REVISED 11 October 2025 ACCEPTED 13 October 2025 PUBLISHED 11 November 2025

CITATION

Lian X-H, Xue H-H, Sun W-J, Chen Y-F, Zeng Z-F, Chen L and Xue J-L (2025) Biomechanical comparison of anterior cervical corpectomy and fusion, anterior controllable antedisplacement and fusion, and anterior cervical X-shape-corpectomy and fusion in the surgical treatment of ossification of the posterior longitudinal ligament: a finite element analysis.

Front. Bioeng. Biotechnol. 13:1594016. doi: 10.3389/fbioe.2025.1594016

COPYRIGHT

© 2025 Lian, Xue, Sun, Chen, Zeng, Chen and Xue. This is an open-access article distributed under the terms of the Creative Commons Attribution License (CC BY). The use. distribution or reproduction in other forums is permitted, provided the original author(s) and the copyright owner(s) are credited and that the original publication in this journal is cited, in accordance with accepted academic practice. No use, distribution or reproduction is permitted which does not comply with these

Biomechanical comparison of anterior cervical corpectomy and fusion, anterior controllable antedisplacement and fusion, and anterior cervical X-shape-corpectomy and fusion in the surgical treatment of ossification of the posterior longitudinal ligament: a finite element analysis

Xiong-Han Lian^{1,2‡}, Huo-Huo Xue^{1‡}, Wen-Jia Sun^{1‡}, Yu-Fan Chen (b) 1‡, Zhi-Feng Zeng 1,2, Liang Chen 3 and Jing-Lai Xue^{1*}

¹Fuzhou Second General Hospital, Fuzhou, China, ²Fujian University of Traditional Chinese Medicine, Fuzhou, China, ³The First Affiliated Hospital of Fujian Medical University, Fuzhou, China

Background: Anterior Cervical Corpectomy and Fusion (ACCF), Anterior Controllable Antedisplacement and Fusion (ACAF), and Anterior Cervical X-Shape-Corpectomy and Fusion (ACXF) have been shown to achieve similar decompression outcomes in the treatment of ossification of the posterior longitudinal ligament. However, the potential biomechanical differences remain unclear.

Methods: Finite element models of the cervical spine (C3-C7) were constructed to simulate ACCF, ACAF, and ACXF. Compare the ranges of motion (ROMs), von Mises stresses in the fixation systems and cortical endplates, and adjacent intervertebral disc pressures (IDPs) under loading conditions.

Results: Postoperatively, ROMs in the fusion area were significantly restricted, with ACAF exhibiting the most severe, followed by ACCF, while ACXF showed the lightest. Peak stresses in the internal fixation systems were highest in ACCF, particularly within the fusion devices. The cages in ACAF experienced lower stress than those in ACXF, whereas the screws showed the opposite trend. ACCF had the highest cortical endplate stresses, while ACXF had the lowest adjacent IDPs.

Conclusion: ACAF and ACXF demonstrate superior biomechanical properties in terms of stability, reduced internal fixation system risk, resistance to subsidence, and lower incidence of adjacent segment disease. As a result, they may serve as viable alternatives to ACCF in certain cases.

KEYWORDS

anterior cervical corpectomy and fusion, anterior controllable antedisplacement and fusion, anterior cervical X-shape-corpectomy and fusion, ossification of the posterior longitudinal ligament, finite element

Introduction

Ossification of the posterior longitudinal ligament (OPLL) was first reported by Key in 1838 and further described in detail by Tsukimoto in 1960 (Hao et al., 2017). The exact pathogenesis of OPLL remains unclear, but it is generally believed to be influenced by genetic and environmental factors. Epidemiological studies indicate that the prevalence of OPLL in the Japanese population aged >20 years ranges from 1.9% to 4.3%, while in Europe and North America, it is between 0.1% and 1.7% (Matsunaga and Sakou, 2012). Approximately 70% of cases occur in the cervical region, with the thoracic and lumbar regions accounting for 15% each (Matsunaga and Sakou, 2012; Saetia et al., 2011; Kawaguchi et al., 2013). C5 is the most commonly affected vertebra (Matsunaga and Sakou, 2012; Saetia et al., 2011; Fujimori et al., 2016; Kawaguchi et al., 2016). Imaging studies have shown that the cervical OPLL (COPLL) detection rate in the Japanese population can be as high as 6.3% (Fujimori et al., 2016) compared to only 1.6% in non-Asian populations (Fujimori et al., 2015).

COPLL can lead to secondary spinal canal stenosis, resulting in compression of the spinal cord. It severely impairs the quality of life and may even result in the loss of the ability to perform activities of daily living. Conservative treatments are frequently ineffective, and follow-up studies have shown that ossification can progress both transversely and longitudinally (Wang et al., 2019). Therefore, surgical intervention is crucial for relieving spinal cord compression, restoring the physiological curvature of the cervical spine, and facilitating neurological recovery (Sun et al., 2020).

Surgical approaches for COPLL are generally classified into anterior and posterior approaches. While anterior surgeries are more technically challenging and carry higher risks, they offer superior decompression and improved postoperative recovery (Feng et al., 2016; Wang et al., 2017). Newer techniques, such as Anterior Controllable Antedisplacement and Fusion (ACAF) and Anterior Cervical X-Shape-Corpectomy and Fusion (ACXF) (Sun et al., 2017; Yang et al., 2018; Liu et al., 2021; Wang H. et al., 2023), are similar to the classic Anterior Cervical Corpectomy and Fusion (ACCF) procedure in that they can remove the ossified tissue in the posterior aspect of the vertebrae to achieve complete decompression.

Abbreviations: OPLL, Ossification of the Posterior Longitudinal Ligament; COPLL, Cervical Ossification of the Posterior Longitudinal Ligament; ACCF, Anterior Cervical Corpectomy and Fusion; ACAF, Anterior Controllable Antedisplacement and Fusion; ACXF, Anterior Cervical X-Shape-Corpectomy and Fusion; FE, Finite Element; IDP, Intervertebral Disc Pressure; ROM, Range of Motion.

However, the biomechanical differences among these approaches remain unclear.

Finite element (FE) analysis is a numerical method that subdivides a structure into finite elements and applies physical laws for simulation and calculation. It has been widely used in biomechanical studies of complex medical scenarios. In this study, the FE model of COPLL was developed to simulate the surgical procedures of ACCF, ACAF, and ACXF. By analyzing the ranges of motion (ROMs), von Mises stresses in internal fixation systems and cortical endplates, and adjacent intervertebral disc pressures (IDPs). This study aims to evaluate the biomechanical effects and provide theoretical insights for clinical practice.

Methods

Establish EF models

The FE model was developed using high-resolution continuous thin-slice CT data from a healthy 52-year-old male volunteer (height: 168 cm; weight: 70 kg; supine position) with no history of spine-related diseases, such as fractures, deformities, or tumors. This study was approved by the Ethics Committee of Fuzhou Second General Hospital, and informed consent was obtained from the volunteer.

First, DICOM-format CT data were imported into Mimics Medical (version 21.0; Materialise Mimics, Leuven, Belgium), where thresholding was applied to extract the bony structures of C3-C7. Next, Geomagic Wrap (version 2021; Geomagic, Research Triangle Park, North Carolina, United States) was used for mesh surface smoothing, and patch SOLIDWORKS (version 2020; Dassault Systems SOLIDWORKS Corp, Waltham, MA, United States) was then employed to model and assemble the cortical bone, trabecular bone, annulus fibrosus, nucleus pulposus, endplate, facet cartilage, and fixation system (the screw: 14 mm long, 3 mm diameter; the titanium mesh: 26 mm high, 10 mm inner diameter, 12 mm outer diameter, cylinder; the titanium plate: $1 \times 14 \times 38$ mm; the cage: $5 \times 14 \times 16$ mm). The intervertebral disc consists of the annulus fibrosus and nucleus pulposus, with a volume ratio of 6:4. Annulus fibers surrounded the ground substance with an inclination to the transverse plane between 15° and 30°, accounting for approximately 19% of the entire annulus fibrosus volume (Zhang J. et al., 2023). The cortical bone, endplate, and facet cartilage were modeled with a thickness of 0.5 mm (Zhang J. et al., 2023; Lin et al., 2024). Finally, springs were used in ANSYS Workbench (version 2022 R2; ANSYS, Pennsylvania, United States) to simulate the ligament complex. All material properties were assumed to be homogeneous and isotropic, with relevant values

TABLE 1 Spinal structure and instrumentation material properties.

Spinal structure and instrumentation	Young's modulus (MPa)	Poisson's ratio	
Vertebral body			
Cortical bone	12,000	0.30	
Cancellous bone	450	0.30	
Endplate	500	0.40	
Intervertebral disc			
Fibers	110	0.30	
Ground substance	4.2	0.49	
Nucleus pulposus	1.0	0.49	
Facet joint cartilage	10.4	0.40	
Ligament			
Anterior longitudinal ligament	10	0.30	
Posterior longitudinal ligament	10	0.30	
Capsular ligament	10	0.30	
Interspinous ligament	1.5	0.30	
Supraspinal ligament	1.5	0.30	
Ligamentum flavum	1.5	0.30	
Implants			
Titanium (plate, screw, and mesh)	110,000	0.30	
PEEK (cage)	3,600	0.30	

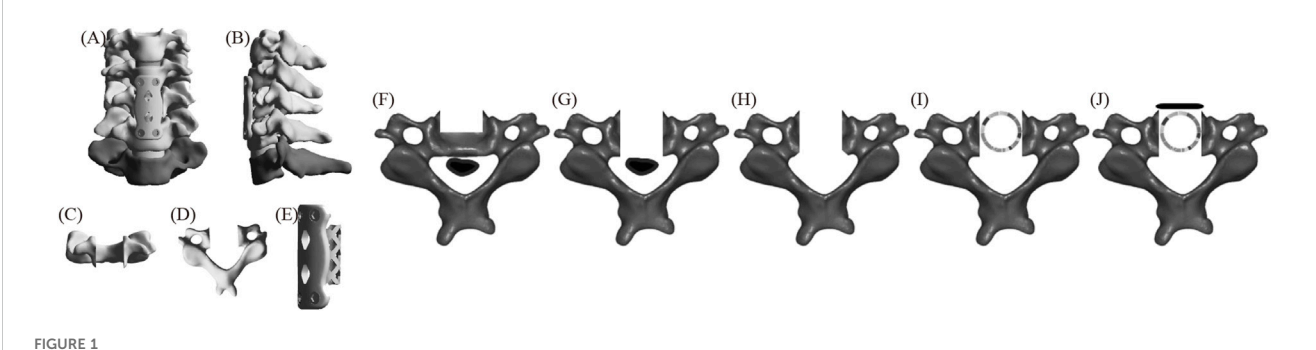


FIGURE 1
The FE model of ACCF (A) positive position; (B) lateral position; (C) C5 positive position; (D) C5 upper position; (E) fixation system; (F–J) C5 surgical procedure.

for Young's modulus and Poisson's ratio provided in Table 1 (Lin et al., 2024; Shen et al., 2022).

Surgical procedures

ACCF

Figure 1 displays the FE model of ACCF. First, the intervertebral discs and cartilage endplates at C4/5 and C5/6 were resected. Subtotal resection of C5 was then performed, followed by

decompression of the ossified tissue. Next, a titanium mesh was installed between C4 and C6, close to the residual vertebrae of C5. Finally, a plate spanning C4-C6 was positioned along the anterior edge and fixed with two screws at the proximal and distal ends, respectively, to ensure stability.

ACAF

Figure 2 displays the FE model of ACAF (Sun et al., 2017). First, the intervertebral discs and cartilage endplates at C4/5 and C5/6 were resected. A slot was then created on the C5 side, and the

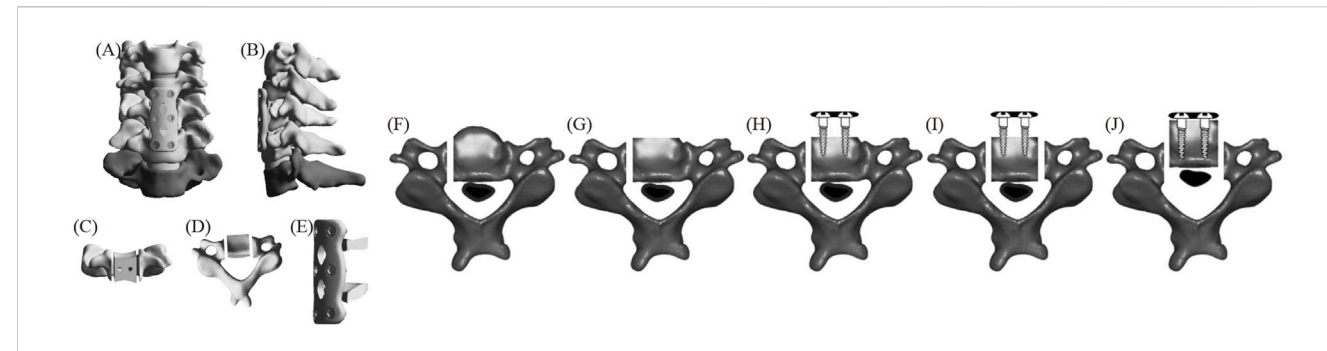


FIGURE 2
The FE model of ACAF (A) positive position; (B) lateral position; (C) C5 positive position; (D) C5 upper position; (E) fixation system; (F–J) C5 surgical procedure.

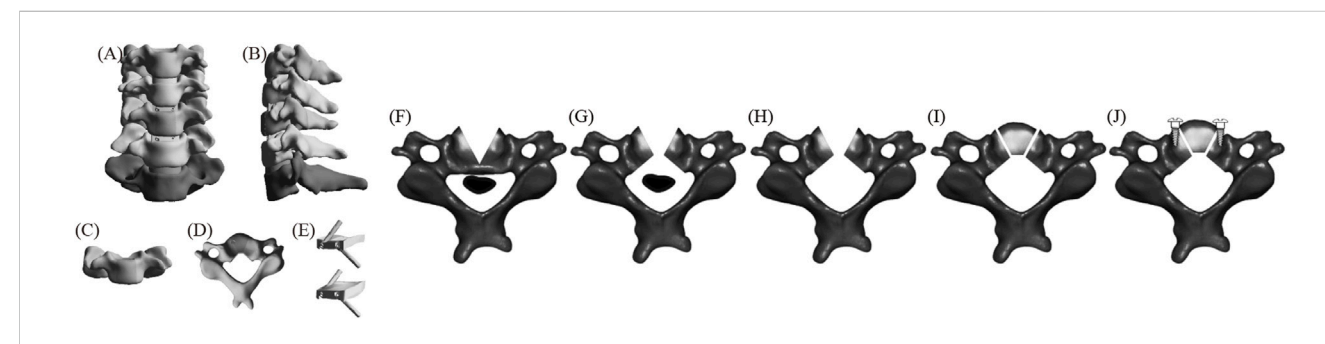


FIGURE 3
The FE model of ACXF (A) positive position; (B) lateral position; (C) C5 positive position; (D) C5 upper position; (E) fixation system; (F–J) C5 surgical procedure.

anterior bone was partially resected. Next, cages were placed at C4/5 and C5/6, respectively. A plate spanning C4-C6 was positioned along the anterior edge and fixed with two screws at each vertebral body. All screws, except at C5, were tightened. Finally, a second slot was created on the opposite side of C5, and the vertebrae-OPLL complex was displaced forward by tightening the screws.

ACXF

Figure 3 displays the FE model of ACXF (Wang H. et al., 2023). First, the intervertebral discs and cartilage endplates at C4/5 and C5/6 were resected. A V-shaped osteotomy was then performed from both sides of C5 towards the center, with the confluence at the posterior part of the vertebral body and the angle between the cross-section and the sagittal plane is approximately 25°. A second inverted V-shaped osteotomy was performed towards the posterior edge of C5. Next, the ossified tissue was removed, and the bone block was transplanted back. Finally, zero-profile cages were installed at C4/5 and C5/6, with two screws inserted obliquely at each level.

Convergence analysis

Convergence analysis is a method of evaluating the accuracy of the FE model by increasing the mesh density to obtain stable results. The percentage changes in the peak von Mises stress were assessed at four different grid sizes (2, 1.5, 1, and 0.5 mm). The final grid size was 1 mm, which satisfied the peak von Mises stress variation range

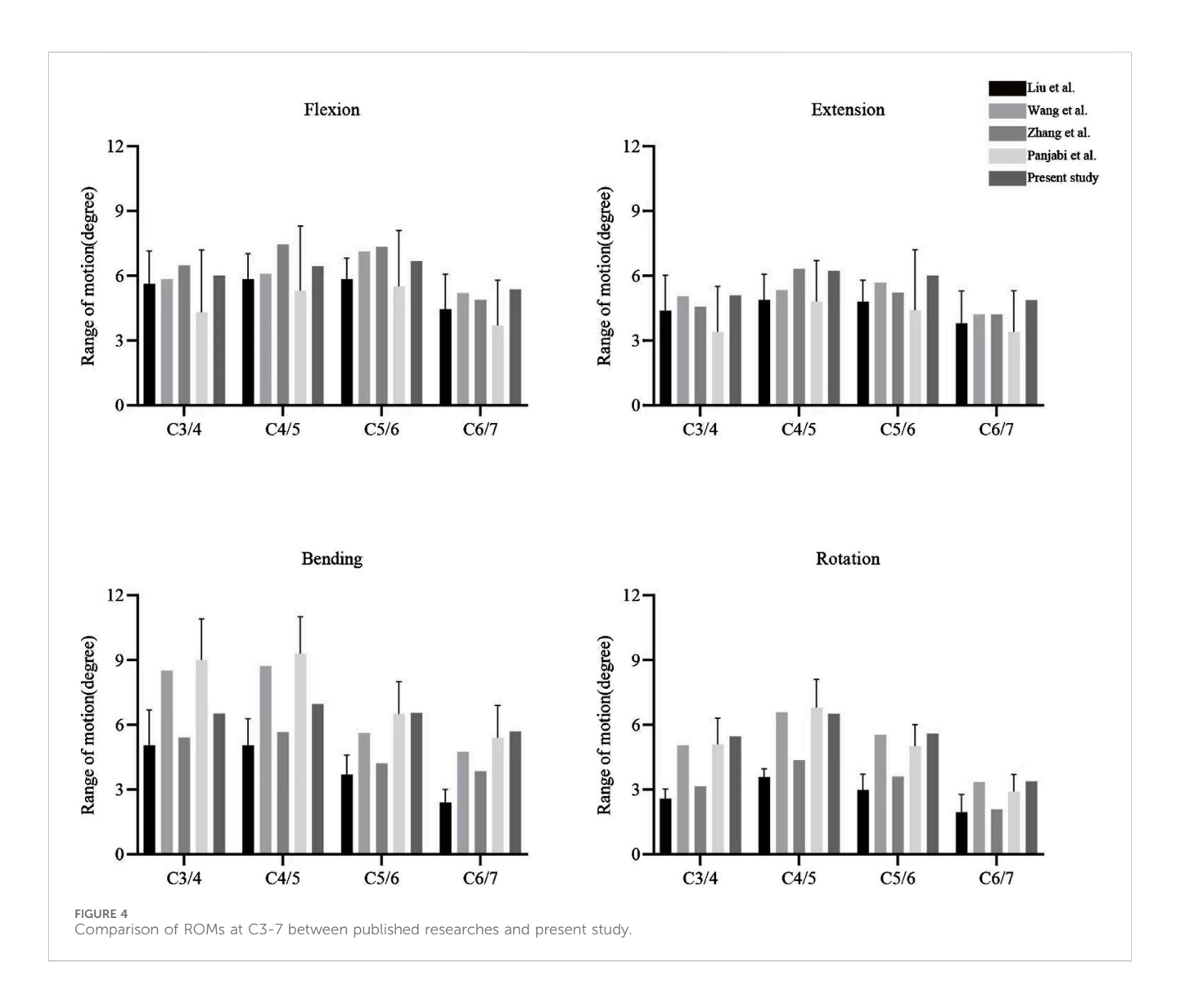
TABLE 2 Convergence analysis results.

Element size	Nodes	Units	Percentage change
2.0 mm	241,351	125,567	>5%
1.5 mm	330,722	175,067	>5%
1.0 mm	589,736	326,699	<5%
0.5 mm	2,601,843	1,617,148	<5%

of <5% while reducing computational cost (Zhang et al., 2022). The relevant data are listed in Table 2.

Contact, boundary, and load conditions

Contact relationships exist between adjacent structures. The articular surfaces of the facet joints are considered frictionless (Zhang J. et al., 2023; Lin et al., 2024; Shen et al., 2022). Tie constraints are applied between the implant system and the cervical spine structures to simulate rigid fusion and ensure adequate osseointegration (Zhang J. et al., 2023; Shen et al., 2022). The model is fixed by constraining the movement of the lower endplate of C7 in all directions, while C3 is unrestricted. A vertical load of 73.6 N is applied to the upper endplate of C3 to simulate the weight of the head, along with a torque of 1.0 Nm to facilitate flexion, extension, lateral bending, and axial rotation (Ahn et al., 2023; Wang H. et al., 2023).



Result

Validity verification

The ROMs of the FE model were compared with published results (Zhang et al., 2022; Wang Y. et al., 2023; Panjabi et al., 2001; Liu et al., 2016). The ROMs at C3/4, C4/5, C5/6, and C6/7 were measured as 6.01°, 6.44°, 6.68°, and 5.37° in flexion; 5.09°, 6.23°, 6.01°, and 4.87° in extension; 6.52°, 6.96°, 6.55°, and 5.69° in lateral bending; and 5.46°, 6.51°, 5.59°, and 3.38° in axial rotation, respectively (Figure 4). These results fell within the standard deviation range reported in previous FE studies and *in vitro* experiments, confirming the validity of the FE model for further analysis.

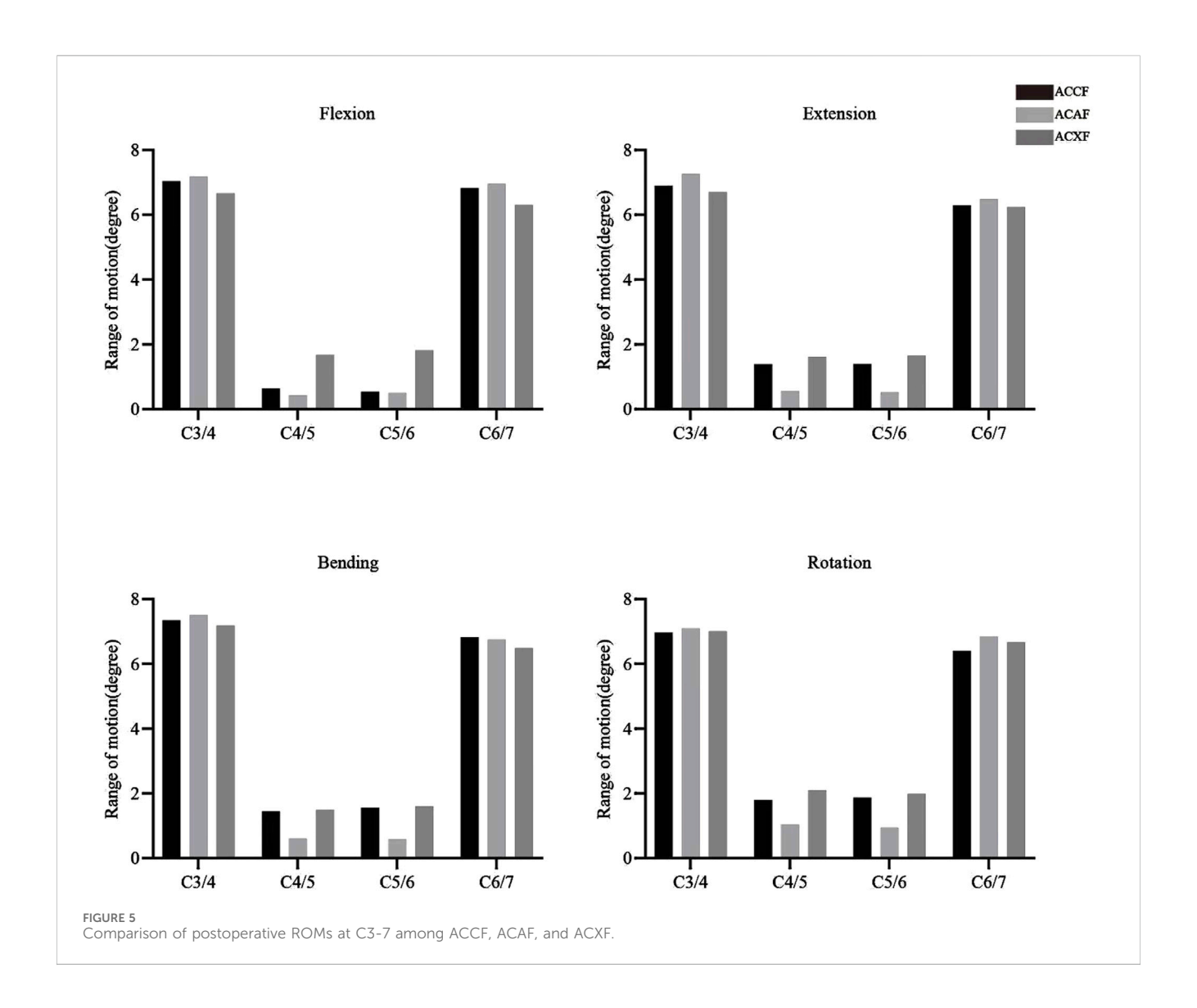
Postoperative ROM

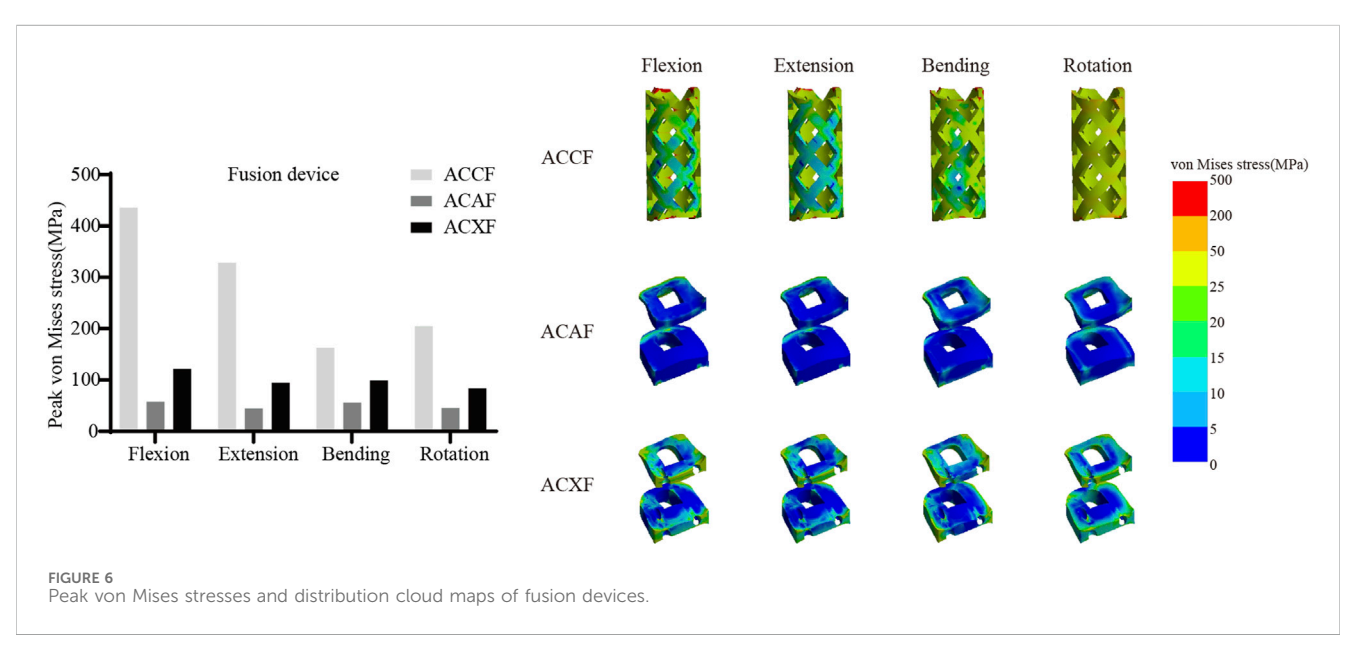
The postoperative ROMs at C4-C6 for ACCF, ACAF, and ACXF were 1.18°, 0.93°, and 3.50° in flexion; 2.79°, 1.09°, and 3.28° in extension; 3.01°, 1.20°, and 3.10° in lateral bending; and 3.68°, 1.99°, and 4.09° in axial rotation, respectively (Figure 5). Among the surgical

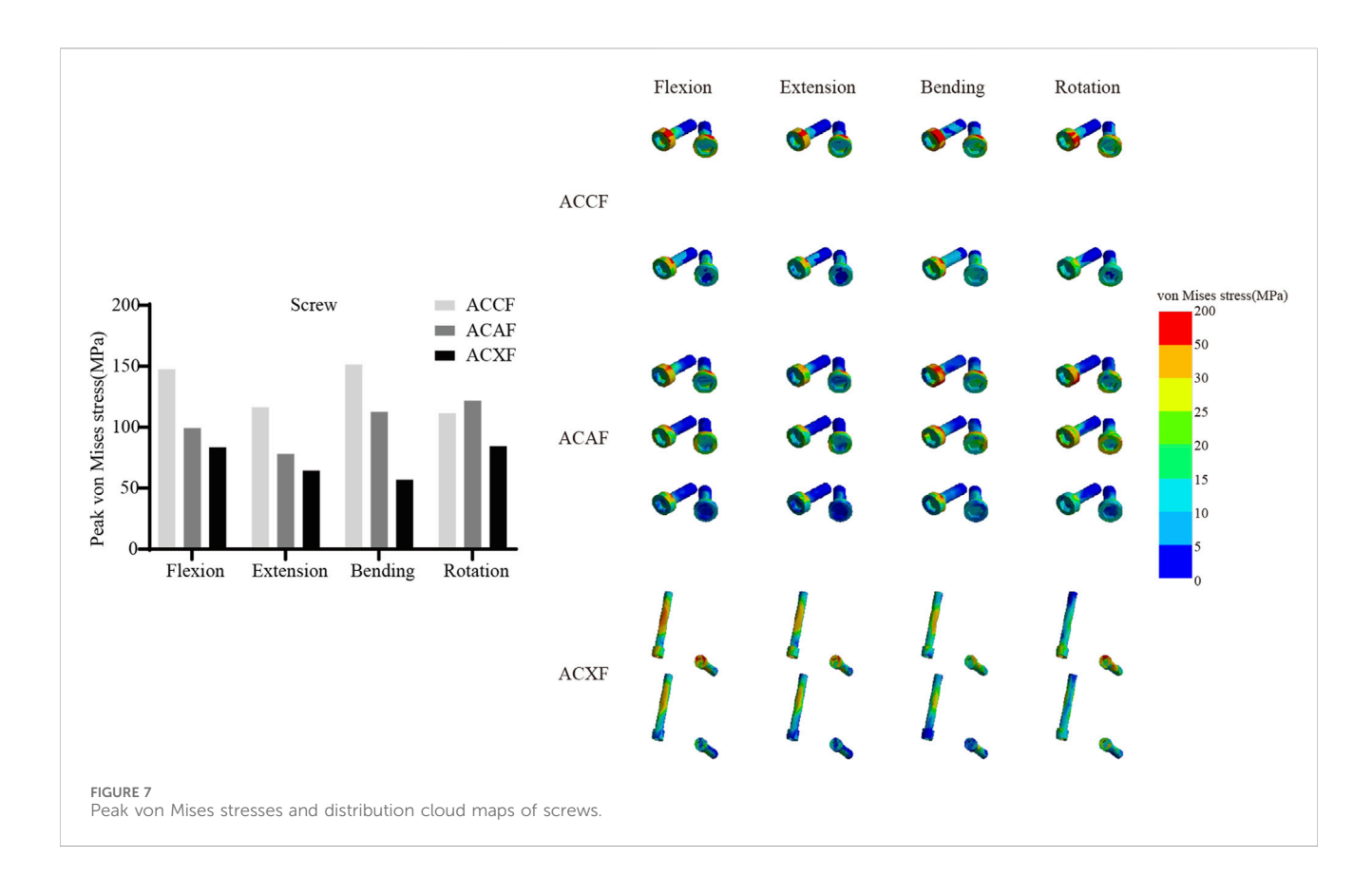
methods, ACXF exhibited the highest ROMs, while ACAF showed the lowest. Motion within the fusion region was significantly restricted. Although adjacent segments exhibited compensatory movements, total ROMs remained lower than preoperative levels.

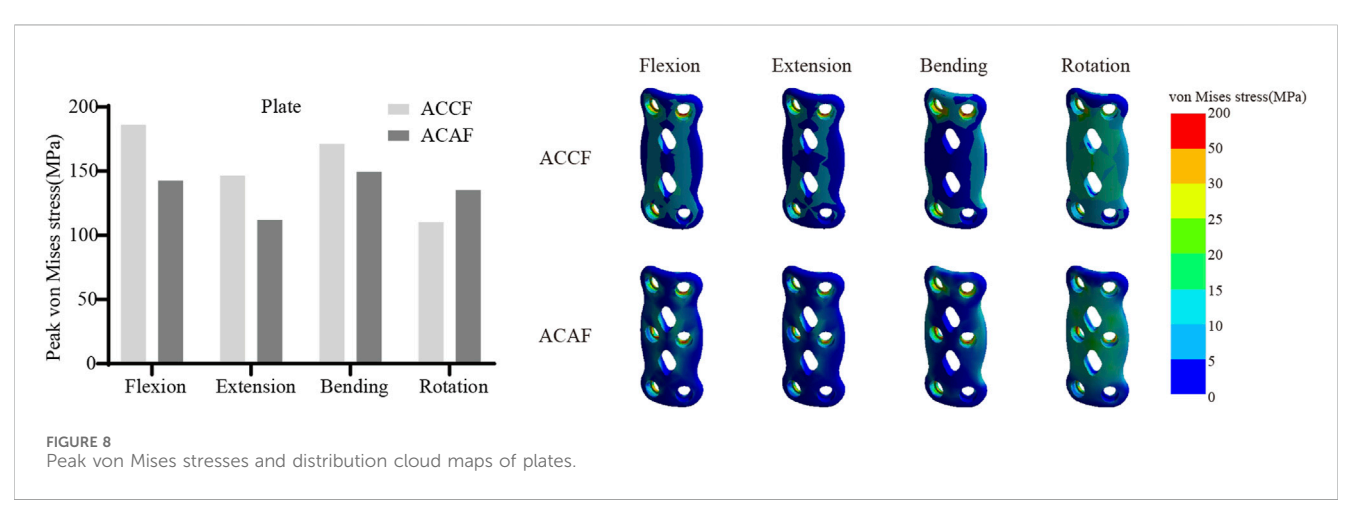
Internal fixation system stress

Figure 6 shows the von Mises stresses in the fusion devices. The peak von Mises stresses for ACCF, ACAF, and ACXF were 435.81 MPa, 57.52 MPa, and 121.42 MPa in flexion; 328.64 MPa, 44.92 MPa, and 94.53 MPa in extension; 162.70 MPa, 55.90 MPa, and 99.15 MPa in lateral bending; and 204.75 MPa, 45.74 MPa, and 83.65 MPa in axial rotation, respectively. Figure 7 shows the von Mises stresses in the screws. The peak von Mises stresses for ACCF, ACAF, and ACXF were 147.64 MPa, 99.29 MPa, and 83.60 MPa in flexion; 116.47 MPa, 78.15 MPa, and 64.46 MPa in extension; 151.40 MPa, 112.50 MPa, and 56.85 MPa in lateral bending; and 111.44 MPa, 121.76 MPa, and 84.40 MPa in axial rotation, respectively. Figure 8 shows the von Mises stresses in the plates. The peak von Mises stresses for ACCF and ACAF were 186.08 MPa and 142.52 MPa in flexion; 146.64 MPa and









112.06 MPa in extension; 171.23 MPa and 149.60 MPa in lateral bending; and 110.24 MPa and 135.29 MPa in axial rotation, respectively. The peak stresses of the plant system within ACCF are the highest, especially in the fusion device. ACAF has the lowest cage stresses, while screws have the lowest stresses in ACXF.

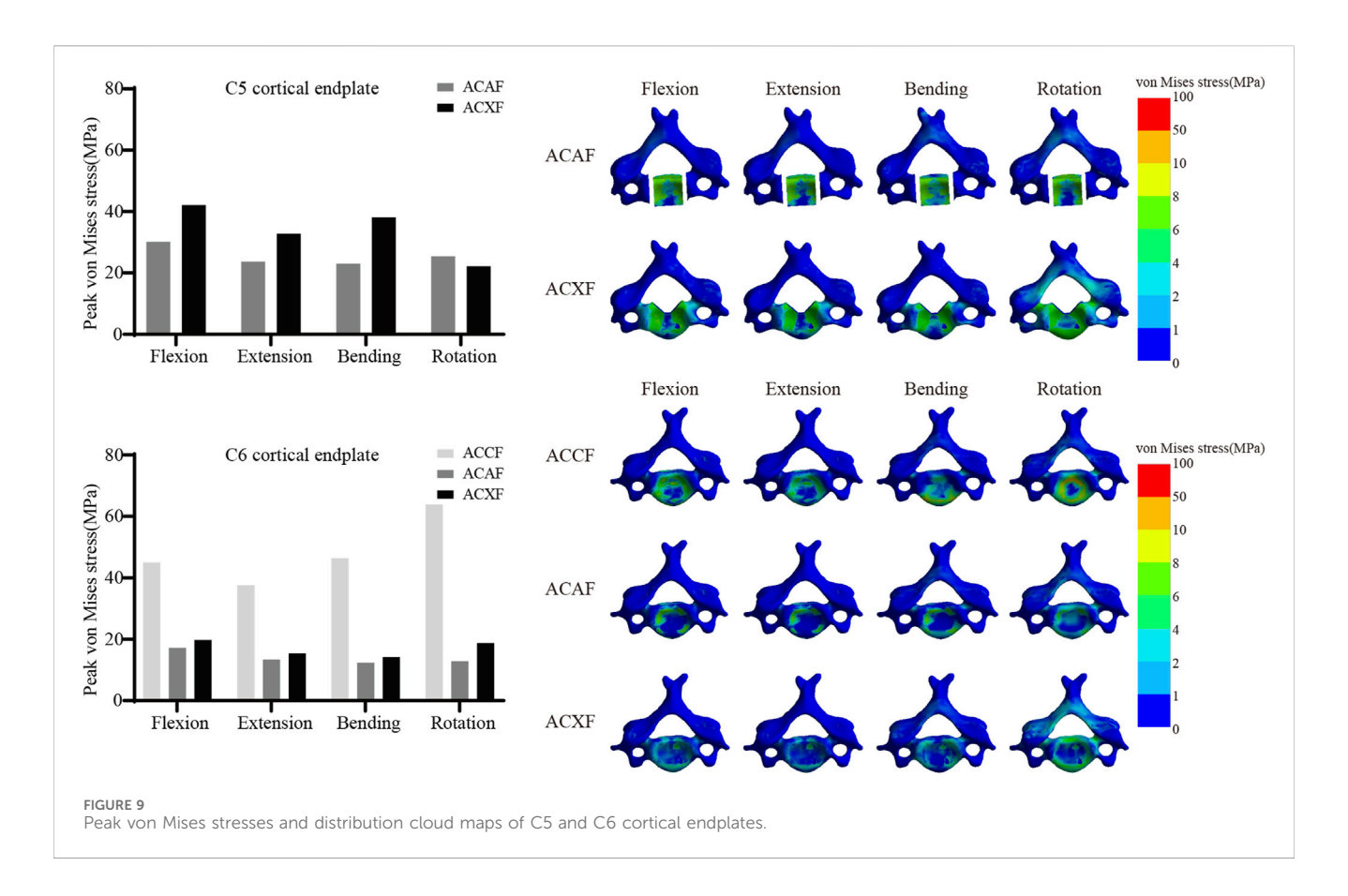
Cortical endplate stress

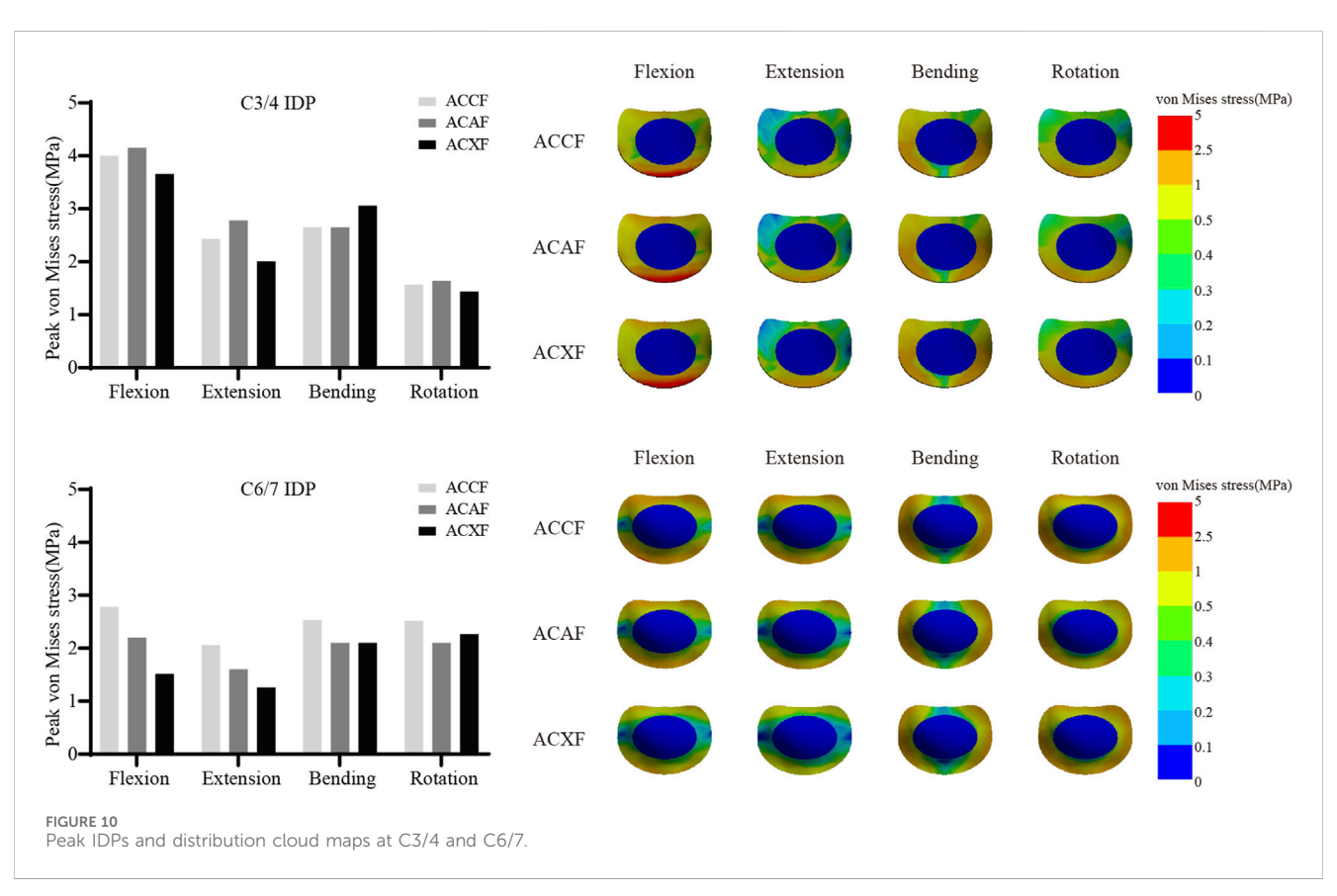
Figure 9 shows the von Mises stresses of C5 and C6 cortical endplates. The peak von Mises stresses on the C5 cortical endplate for ACAF and ACXF were 30.19 MPa and 42.11 MPa in flexion, 23.73 MPa and 32.77 MPa in extension, 23.06 MPa and 38.13 MPa in

lateral bending, and 25.44 MPa and 22.16 MPa in axial rotation, respectively. The peak von Mises stresses on the C6 cortical endplate for ACCF, ACAF, and ACXF were 45.03 MPa, 17.20 MPa, and 19.74 MPa in flexion; 37.63 MPa, 13.36 MPa, and 15.45 MPa in extension; 46.43 MPa, 12.35 MPa, and 14.22 MPa in lateral bending; and 63.87 MPa, 12.86 MPa, and 18.76 MPa in axial rotation, respectively.

Intervertebral disc pressure

Figure 10 shows the IDPs at C3/4 and C6/7. The peak IDPs at C3/4 for ACCF, ACAF, and ACXF were 4.00 MPa, 4.15 MPa, and 3.66 MPa in flexion; 2.43 MPa, 2.78 MPa, and 2.01 MPa in extension;





2.67 MPa, 2.65 MPa, and 3.06 MPa in lateral bending; and 1.57 MPa, 1.64 MPa, and 1.44 MPa in axial rotation, respectively. The peak IDPs at C6/7 for ACCF, ACAF, and ACXF were 2.78 MPa, 2.20 MPa, and 1.52 MPa in flexion; 2.06 MPa, 1.60 MPa, and 1.26 MPa in extension; 2.53 MPa, 2.10 MPa, and 2.08 MPa in lateral bending; and 2.52 MPa, 2.10 MPa, and 2.27 MPa in axial rotation, respectively.

Discussion

FE analysis, through three-dimensional reconstruction and material modeling, enables the simulation of skeletal stress distribution, joint biomechanics, and prosthesis-bone interface interactions, providing a foundation for personalized surgical planning. Traditionally, for COPLL involving the entire posterior vertebral body, ACCF or posterior approaches were the only viable options. ACXF allows direct exposure and resection of the posterior ossified mass, while ACAF indirectly decompresses the spinal cord by lifting the vertebrae-OPLL complex. Given that both ACAF and ACXF achieve a decompression range comparable to ACCF, they share similar surgical indications, thereby expanding clinical treatment options. This study aims to establish FE models of ACCF, ACAF, and ACXF to investigate potential biomechanical differences, providing insights to inform surgical decision-making.

Construct stability

ROM is commonly used in FE analysis to objectively assess model stability, with smaller deformations under loading conditions indicating superior performance. As expected, all three surgical models exhibited significantly restricted ROMs compared to the preoperative state, while adjacent segments demonstrated compensatory motion, consistent with previous findings in spinal fusion research (Lin et al., 2024; Shen et al., 2022; Zhang et al., 2022; Wang Y. et al., 2023; Wo et al., 2021). Compared to ACCF, our study found that ACAF led to a more pronounced reduction in ROMs across all directions, aligning with Kong's FE studies (Kong et al., 2024). This is likely due to ACAF preserving more of the vertebral structure, thereby enhancing the intrinsic mechanical stability of the cervical spine. Both ACAF and ACXF avoid subtotal corpectomy, maintaining spinal structural integrity. Structurally, ACAF utilizes a twolevel cage-plate system, whereas ACXF employs a two-level zero-profile system. Multiple studies have reported greater ROM in the zero-profile system compared to the cage-plate system (Panchal et al., 2019; Salari et al., 2022; Zhang X. et al., 2023). Consistently, our results indicate that ACXF exhibits greater ROMs than ACAF, possibly due to the anterior plate in ACXF. Given its ability to maximize vertebral preservation while providing strong internal fixation, ACAF may be a preferable option for patients with compromised baseline cervical stability, such as those with severe osteoporosis, weakened paraspinal musculature, or altered cervical alignment.

Risks of instrument-related complications

Implant-related complications, including fracture, loosening, and displacement, may result in neck pain, dysphagia, or spinal cord

compression, potentially necessitating revision surgery. The peak von Mises stress within the internal fixation system serves as an indicator of mechanical failure risk. It is noteworthy that the screw stresses in ACAF are higher than those in ACXF, whereas the opposite trend is observed for the fusion device. This discrepancy can be attributed to the distinct fixation structures of the two techniques. In ACAF, the plate-screw construct functions as a load-sharing bridge, redistributing axial forces and thereby increasing screw stresses while reducing the stress borne by the cage. In contrast, ACXF relies on zero-profile cages without supplement; the screws in this construct primarily serve as anchors to secure the cage rather than as load-bearing elements. Consequently, the cage in ACXF directly assumes the majority of the axial load transmission, which explains the relatively lower screw stresses but higher stresses within the fusion device. Our study found that ACCF exhibited the highest peak stresses within the fixation system, likely due to the extensive vertebral resection and increased load-bearing demands placed on the implants for structural reconstruction. Clinical followup studies have reported implant-related complications following ACCF, whereas no such cases have been documented for ACAF or ACXF to date (Wang Y. et al., 2023; Kong et al., 2024). However, this may be attributed to the limited number of cases and short follow-up duration. Further clinical studies are needed to validate these findings.

Bone fusion

The internal fixation system plays a crucial role in maintaining early postoperative stability. Effective bony fusion is essential for successful surgery, and fusion rate is a key metric for clinical evaluation. According to Wolff's law (Frost, 2004), bone formation is optimal when mechanical stress is maintained within the range of 2–60 MPa; stress levels that are too low may lead to bone resorption, while excessive stress can result in bone damage. Stress distribution maps indicate favorable loading patterns across the cortical endplates in ACCF, ACAF, and ACXF, consistent with clinical studies reporting no significant differences in fusion rates among the three techniques within 1 year (Sun et al., 2017; Wang Y. et al., 2023). A region of low stress is observed at the center of the cortical endplate, emphasizing the importance of adequate bone grafting within the fusion construct to ensure sufficient mechanical stimulus for bone growth.

Subsidence resistance

Subsidence is a common complication following spinal fusion, often attributed to factors such as osteoporosis, endplate damage, cancellous bone exposure, and microfractures. Our analysis revealed that ACCF exhibited the highest cortical endplate stresses, consistent with clinical findings that titanium mesh cages have a higher subsidence rate than interbody cages (Chen et al., 2023; Lee et al., 2021), which is related to the greater load-bearing demands and smaller contact surface. Zhang proposed a novel anatomical titanium mesh cage with integrated spacers (Zhang et al., 2022), which theoretically offers superior biomechanical performance and may represent a promising clinical alternative. Xu compared subsidence across seven cervical fusion systems (Xu et al., 2020), including standalone cage constructs, cageplate constructs, and zero-profile systems. Their findings demonstrated

that the addition of an anterior plate significantly improves resistance to subsidence, which may explain the lower cortical endplate stresses observed in ACAF compared to ACXF. Additionally, within the same surgical approach, the C5 cortical endplate exhibited greater stresses than C6, likely due to osteotomy-induced disruption of vertebral integrity. The preservation of bony structures plays a crucial role in maintaining resistance to deformation.

Adjacent segment degeneration

Postoperative increases in adjacent segment ROM can lead to further compression or stretching of the intervertebral disc, elevating IDPs and accelerating adjacent segment disease. Among the three surgical models, ACXF demonstrated the lowest adjacent segment IDPs. Notably, ACXF also imposed the least restriction on fusion segment ROMs, which may indirectly reduce compensatory motion at adjacent levels. This finding aligns with previous meta-analyses (Guo et al., 2021; Kahaer et al., 2022; Liu et al., 2022; Chen et al., 2024), which reported a lower risk of adjacent segment disease in zero-profile systems compared to cage-plate constructs. Ouyang did not observe significant differences in the adjacent segment IDPs between the single-level mesh-plate system and the two-level cage-plate system (Ouyang et al., 2020). This further verifies the results and emphasizes the advantages of ACXF in preventing adjacent segment disease. Consistent with prior FE studies (Zhang X. et al., 2023; Zhang et al., 2022), our results show that IDPs are primarily concentrated in the annulus fibrosus, with a distribution pattern corresponding to the direction of movement. The cellular and biomechanical responses of the annulus fibrosus under high stress may provide further insights into intervertebral disc degeneration.

Limitation

Currently, FE analysis is widely used in biomechanics research, offering valuable insights for both basic medical science and clinical applications. However, this study has several limitations. First, the cervical spine model was based on CT data from a healthy volunteer and may not fully reflect degenerative changes in OPLL patients, including osteoporosis, osteophyte formation, small joint disorders, intervertebral disc aging, and ligament degeneration, etc. Second, most ligaments were modeled as spring elements, which cannot accurately reflect the stiffness and restraint effects of ossified lesions. Third, the simplified cervical spine and implant system may not fully replicate the in vivo biomechanical environment. Fourth, most contact interactions in the FE model were defined as tied connections, potentially overlooking certain micromovements. Finally, we acknowledge that ACAF is often clinically indicated for multilevel OPLL, whereas this study simulated only a single-segment model. The biomechanical behavior of multilevel constructs may differ from that of a single-level procedure. A previous FE study comparing single- and two-level anterior cervical discectomy and fusion found that, after adding additional segments, the biomechanical differences between zero-profile and cage-plate systems not only persisted but were further amplified (Hua et al., 2020). Multilevel studies are therefore warranted to achieve a more comprehensive understanding of biomechanical performance in clinical practice. Thus, this study aims to identify biomechanical trends rather than establish definitive conclusions.

Conclusion

The risks associated with internal fixation in ACAF and ACXF are relatively low, with both approaches demonstrating strong resistance to subsidence. ACAF provides superior overall stability and may therefore be more suitable for patients with poor cervical stability, such as those with severe degenerative changes or osteoporosis. In contrast, ACXF is associated with a lower risk of adjacent segment disease and may be preferable for younger patients who require preservation of cervical mobility over the long term. Taken together, these findings suggest that both ACAF and ACXF can serve as preferable alternatives to ACCF, and surgical strategies should be tailored to individual patient characteristics.

Data availability statement

The original contributions presented in the study are included in the article/supplementary material, further inquiries can be directed to the corresponding author.

Ethics statement

The studies involving humans were approved by Ethics Committee of Fuzhou Second General Hospital. The studies were conducted in accordance with the local legislation and institutional requirements. The participants provided their written informed consent to participate in this study. Written informed consent was obtained from the individual(s) for the publication of any potentially identifiable images or data included in this article.

Author contributions

X-HL: Writing - original draft, Supervision, Writing - review and editing, Project administration, Data curation, Methodology, Formal Analysis, Visualization, Validation, Software. H-HX: Data curation, Validation, Visualization, Writing - review and editing, Writing - original draft, Supervision, Formal Analysis, Software. W-JS: Writing - original draft, Software, Visualization, Data curation. Y-FC: Visualization, Data curation, Software, Writing - original draft. Z-FZ: Writing - original draft, Visualization, Resources, Investigation. LC: Investigation, Resources, Visualization, Writing – original draft. J-LX: Methodology, Validation, Formal Analysis, Project administration, Supervision, Data curation, Conceptualization, Resources. Writing - review and editing, Funding acquisition.

Funding

The author(s) declare that financial support was received for the research and/or publication of this article. This study was supported by the Fujian Provincial Natural Science Foundation Project (Grant

No. 2022J011312). This study was also supported by the Fujian Provincial Clinical Medical Research Center for First Aid and Rehabilitation in Orthopaedic Trauma (Grant No. 2020Y2014).

Acknowledgements

Thank the volunteer for providing imaging data for our research. Thank Jian-gang Shi and Hao Liu for designing and implementing the ACAF and ACXF, respectively. Thank Fuzhou Second General Hospital and Fujian University of Traditional Chinese Medicine for their assistance and cooperation.

Conflict of interest

The authors declare that the research was conducted in the absence of any commercial or financial relationships that could be construed as a potential conflict of interest.

References

Ahn, C.-H., Kang, S., Cho, M., Kim, S.-H., Kim, C. H., Han, I., et al. (2023). Comparing zero-profile and conventional cage and plate in anterior cervical discectomy and fusion using finite-element modeling. *Sci. Rep.* 13 (1), 15766. doi:10. 1038/s41598-023-43086-x

Chen, T., Wang, Y., Zhou, H., Lin, C., Li, X., Yang, H., et al. (2023). Comparison of anterior cervical discectomy and fusion versus anterior cervical corpectomy and fusion in the treatment of localized ossification of the posterior longitudinal ligament. J. Orthop. Surg. Hong Kong 31 (1), 10225536231167704. doi:10.1177/10225536231167704

Chen, L., Liu, D., Wang, M., Huang, Y., and Chen, Z. (2024). Anterior cervical discectomy and fusion with zero-profile anchored spacer Versus plate and cage for 3-Level contiguous cervical degenerative disease A systematic review and meta-analysis. *World Neurosurg.* 190 (10), 228–239. doi:10.1016/j.wneu.2024.07.102

Feng, F., Ruan, W., Liu, Z., Li, Y., and Cai, L. (2016). Anterior versus posterior approach for the treatment of cervical compressive myelopathy due to ossification of the posterior longitudinal ligament: a systematic review and meta-analysis. *Int. J. Surg.* 27, 26–33. doi:10.1016/j.ijsu.2016.01.038

Frost, H. M. (2004). A 2003 update of bone physiology and Wolff's law for clinicians. Angle Orthod. 74 (1), 3–15. doi:10.1043/0003-3219(2004)074<0003:AUOBPA>2.0. CO;2

Fujimori, T., Le, H., Hu, S. S., Chin, C., Pekmezci, M., Schairer, W., et al. (2015). Ossification of the posterior longitudinal ligament of the cervical spine in 3161 patients. Spine 40 (7), E394–E403. doi:10.1097/brs.0000000000000791

Fujimori, T., Watabe, T., Iwamoto, Y., Hamada, S., Iwasaki, M., and Oda, T. (2016). Prevalence, concomitance, and distribution of ossification of the spinal ligaments. *Spine* 41 (21), 1668–1676. doi:10.1097/brs.00000000001643

Guo, Z., Wu, X., Yang, S., Liu, C., Zhu, Y., Shen, N., et al. (2021). Anterior cervical discectomy and fusion using Zero-P system for treatment of cervical spondylosis: a meta-analysis. *Pain Res. Manag.* 2021, 1–15. doi:10.1155/2021/3960553

Hao, D., Lv, S., He, B., Liu, Y., Gao, R., and Yan, L. (2017). The pathogenesis of ossification of the posterior longitudinal ligament. *Aging Dis.* 8 (5), 570–582. doi:10. 14336/ad.2017.0201

Hua, W., Zhi, J., Ke, W., Wang, B., Yang, S., Li, L., et al. (2020). Adjacent segment biomechanical changes after one- or two-level anterior cervical discectomy and fusion using either a zero-profile device or cage plus plate: a finite element analysis. *Comput. Biol. Med.* 120, 103760. doi:10.1016/j.compbiomed.2020.103760

Kahaer, A., Chen, R., Maitusong, M., Mijiti, P., and Rexiti, P. (2022). Zero-profile implant versus conventional cage-plate construct in anterior cervical discectomy and fusion for the treatment of single-level degenerative cervical spondylosis: a systematic review and meta-analysis. *J. Orthop. Surg. Res.* 17 (1), 506. doi:10.1186/s13018-022-02397.0

Kawaguchi, Y., Nakano, M., Yasuda, T., Seki, S., Hori, T., and Kimura, T. (2013). Ossification of the posterior longitudinal ligament in not only the cervical spine, but also other spinal regions. *Spine* 38 (23), E1477–E1482. doi:10.1097/BRS.0b013e3182a54f00

Kawaguchi, Y., Nakano, M., Yasuda, T., Seki, S., Hori, T., Suzuki, K., et al. (2016). Characteristics of ossification of the spinal ligament; incidence of ossification of the

Generative AI statement

The author(s) declare that no Generative AI was used in the creation of this manuscript.

Any alternative text (alt text) provided alongside figures in this article has been generated by Frontiers with the support of artificial intelligence and reasonable efforts have been made to ensure accuracy, including review by the authors wherever possible. If you identify any issues, please contact us.

Publisher's note

All claims expressed in this article are solely those of the authors and do not necessarily represent those of their affiliated organizations, or those of the publisher, the editors and the reviewers. Any product that may be evaluated in this article, or claim that may be made by its manufacturer, is not guaranteed or endorsed by the publisher.

ligamentum flavum in patients with cervical ossification of the posterior longitudinal ligament – analysis of the whole spine using multidetector CT. *J. Orthop. Sci.* 21 (4), 439–445. doi:10.1016/j.jos.2016.04.009

Kong, Q., Li, F., Yan, C., Sun, J., Sun, P., Ou-Yang, J., et al. (2024). Biomechanical comparison of anterior cervical corpectomy decompression and fusion, anterior cervical discectomy and fusion, and anterior controllable antedisplacement and fusion in the surgical treatment of multilevel cervical spondylotic myelopathy: a finite element analysis. *Orthop. Surg.* 16 (3), 687–699. doi:10.1111/os.13994

Lee, D. H., Park, S., Hong, C. G., Park, K. B., Cho, J. H., Hwang, C. J., et al. (2021). Fusion and subsidence rates of vertebral body sliding osteotomy: Comparison of 3 reconstructive techniques for multilevel cervical myelopathy. *Spine J.* 21 (7), 1089–1098. doi:10.1016/j.spinee.2021.03.023

Lin, Z., Lin, D., Xu, L., Chen, Q., Vashisth, M. K., Huang, X., et al. (2024). Biomechanical evaluation on a new type of vertebral titanium porous mini-plate and mechanical comparison between cervical open-door laminoplasty and laminectomy: a finite element analysis. *Front. Bioeng. Biotechnol.* 12, 1353797. doi:10.3389/fbioe.2024.1353797

Liu, Q., Guo, Q., Yang, J., Zhang, P., Xu, T., Cheng, X., et al. (2016). Subaxial cervical intradiscal pressure and segmental kinematics following atlantoaxial fixation in different angles. *World Neurosurg.* 87, 521–528. doi:10.1016/j.wneu.2015.09.025

Liu, Y., Meng, Y., Liu, H., Ding, C., Wang, B., and Hong, Y. (2021). A novel anterior cervical X-Shape-Corpectomy and fusion for cervical spinal stenosis at C4-C6 level: a technical note. *World Neurosurg.* 149, 181–189. doi:10.1016/j.wneu. 2021.02.098

Liu, Z., Yang, Y., Lan, J., Xu, H., Zhang, Z., and Miao, J. (2022). Changes in cervical alignment of Zero-profile device versus conventional cage-plate construct after anterior cervical discectomy and fusion: a meta-analysis. *J. Orthop. Surg. Res.* 17 (1), 510. doi:10. 1186/s13018-022-03400-1

Matsunaga, S., and Sakou, T. (2012). Ossification of the posterior longitudinal ligament of the cervical spine. *Spine* 37 (5), E309–E314. doi:10.1097/BRS. 0b013e318241ad33

Ouyang, P., Li, J., He, X., Dong, H., Zang, Q., Li, H., et al. (2020). Biomechanical comparison of 1-Level corpectomy and 2-Level discectomy for cervical spondylotic myelopathy: a finite element analysis. *Med. Sci. Monit.* 26, e919270. doi:10.12659/MSM. 919270

Panchal, R., Gandhi, A., Ferry, C., Farmer, S., Hansmann, J., and Wanebo, J. (2019). A biomechanical evaluation of a next-generation integrated and modular ACDF device possessing full-plate, half-plate, and No-Profile fixation iterations. *Glob. Spine J.* 9 (8), 826–833. doi:10.1177/2192568219834252

Panjabi, M. M., Crisco, J. J., Vasavada, A., Oda, T., Cholewicki, J., Nibu, K., et al. (2001). Mechanical properties of the human cervical spine as shown by three-dimensional load-displacement curves. *Spine* 26 (24), 2692–2700. doi:10.1097/00007632-200112150-00012

Saetia, K., Cho, D., Lee, S., Kim, D. H., and Kim, S. D. (2011). Ossification of the posterior longitudinal ligament: a review. *Neurosurg. Focus* 30 (3), E1. doi:10.3171/2010. 11.Focus10276

Salari, N., Konz, G., Ferry, C., Gandhi, A., Freeman, A., Davis, R., et al. (2022). Anterior cervical discectomy and fusion with a No-Profile integrated fixation allograft device: an *in vitro* biomechanical analysis and clinical case series. *Int. J. Spine Surg.* 16 (2), 247–255. doi:10.14444/8224

- Shen, Y.-W., Yang, Y., Liu, H., Qiu, Y., Li, M., Ma, L.-T., et al. (2022). Biomechanical evaluation of intervertebral fusion process after anterior cervical discectomy and fusion: a finite element study. *Front. Bioeng. Biotechnol.* 10, 842382. doi:10.3389/fbioe.2022. 842382
- Sun, J., Shi, J., Xu, X., Yang, Y., Wang, Y., Kong, Q., et al. (2017). Anterior controllable antidisplacement and fusion surgery for the treatment of multilevel severe ossification of the posterior longitudinal ligament with myelopathy: preliminary clinical results of a novel technique. *Eur. Spine J.* 27 (6), 1469–1478. doi:10.1007/s00586-017-5437-4
- Sun, X., Wang, Y., Sun, J., Xu, X., Kong, Q., Chen, Y., et al. (2020). Consensus statement on diagnosis and treatment of cervical ossification of posterior longitudinal ligament from asia pacific spine society (APSS) 2020. *J. Orthop. Surg.* 28 (3), 2309499020975213. doi:10.1177/2309499020975213
- Wang, S., Xiang, Y., Wang, X., Li, H., Hou, Y., Zhao, H., et al. (2017). Anterior corpectomy comparing to posterior decompression surgery for the treatment of multi-level ossification of posterior longitudinal ligament: a meta-analysis. *Int. J. Surg.* 40, 91–96. doi:10.1016/j.ijsu.2017.02.058
- Wang, L., Jiang, Y., Li, M., and Qi, L. (2019). Postoperative progression of cervical ossification of posterior longitudinal ligament: a systematic review. *World Neurosurg.* 126, 593–600. doi:10.1016/j.wneu.2019.03.229
- Wang, H., Liu, Y., Wu, T., Yan, C., He, J., Huang, K., et al. (2023). Anterior cervical X-shape-corpectomy and fusion vs. anterior cervical corpectomy and fusion for two-level cervical spondylosis. *Eur. Spine J.* 33 (1), 205–215. doi:10.1007/s00586-023-07986-w

- Wang, Y., Liu, Y., Zhang, A., Han, Q., Jiao, J., Chen, H., et al. (2023). Biomechanical evaluation of a novel individualized zero-profile cage for anterior cervical discectomy and fusion: a finite element analysis. *Front. Bioeng. Biotechnol.* 11, 1229210. doi:10.3389/fbioe.2023.1229210
- Wo, J., Lv, Z., Wang, J., Shen, K., Zhu, H., Liu, Y., et al. (2021). Biomechanical analysis of cervical artificial disc replacement using cervical subtotal discectomy prosthesis. *Front. Bioeng. Biotechnol.* 9, 680769. doi:10.3389/fbioe.2021.680769
- Xu, J., He, Y., Li, Y., Lv, G.-H., Dai, Y.-L., Jiang, B., et al. (2020). Incidence of subsidence of seven intervertebral devices in anterior cervical discectomy and fusion: a network meta-analysis. *World Neurosurg*. 141, 479–489.e4. doi:10.1016/j.wneu.2020.
- Yang, H., Sun, J., Shi, J., Shi, G., Guo, Y., and Yang, Y. (2018). Anterior controllable antedisplacement fusion (ACAF) for severe cervical ossification of the posterior longitudinal ligament: Comparison with anterior cervical corpectomy with fusion (ACCF). *World Neurosurg.* 115, e428–e436. doi:10.1016/j.wneu.2018.04.065
- Zhang, K., Yang, Y., Ma, L., Qiu, Y., Wang, B., Ding, C., et al. (2022). Biomechanical effects of a novel anatomic titanium mesh cage for single-level anterior cervical corpectomy and fusion: a finite element analysis. *Front. Bioeng. Biotechnol.* 10, 881979. doi:10.3389/fbioe.2022.881979
- Zhang, J., Chen, W., Weng, R., Liang, D., Jiang, X., and Lin, H. (2023). Biomechanical effect of endplate defects on the intermediate vertebral bone in consecutive two-level anterior cervical discectomy and fusion: a finite element analysis. *BMC Musculoskelet. Disord.* 24 (1), 407. doi:10.1186/s12891-023-06453-3
- Zhang, X., Yang, Y., Shen, Y.-W., Zhang, K.-R., Ma, L.-T., Ding, C., et al. (2023). Biomechanical performance of the novel assembled uncovertebral joint fusion cage in single-level anterior cervical discectomy and fusion: a finite element analysis. *Front. Bioeng. Biotechnol.* 11, 931202. doi:10.3389/fbioe.2023.931202